SFigure 1

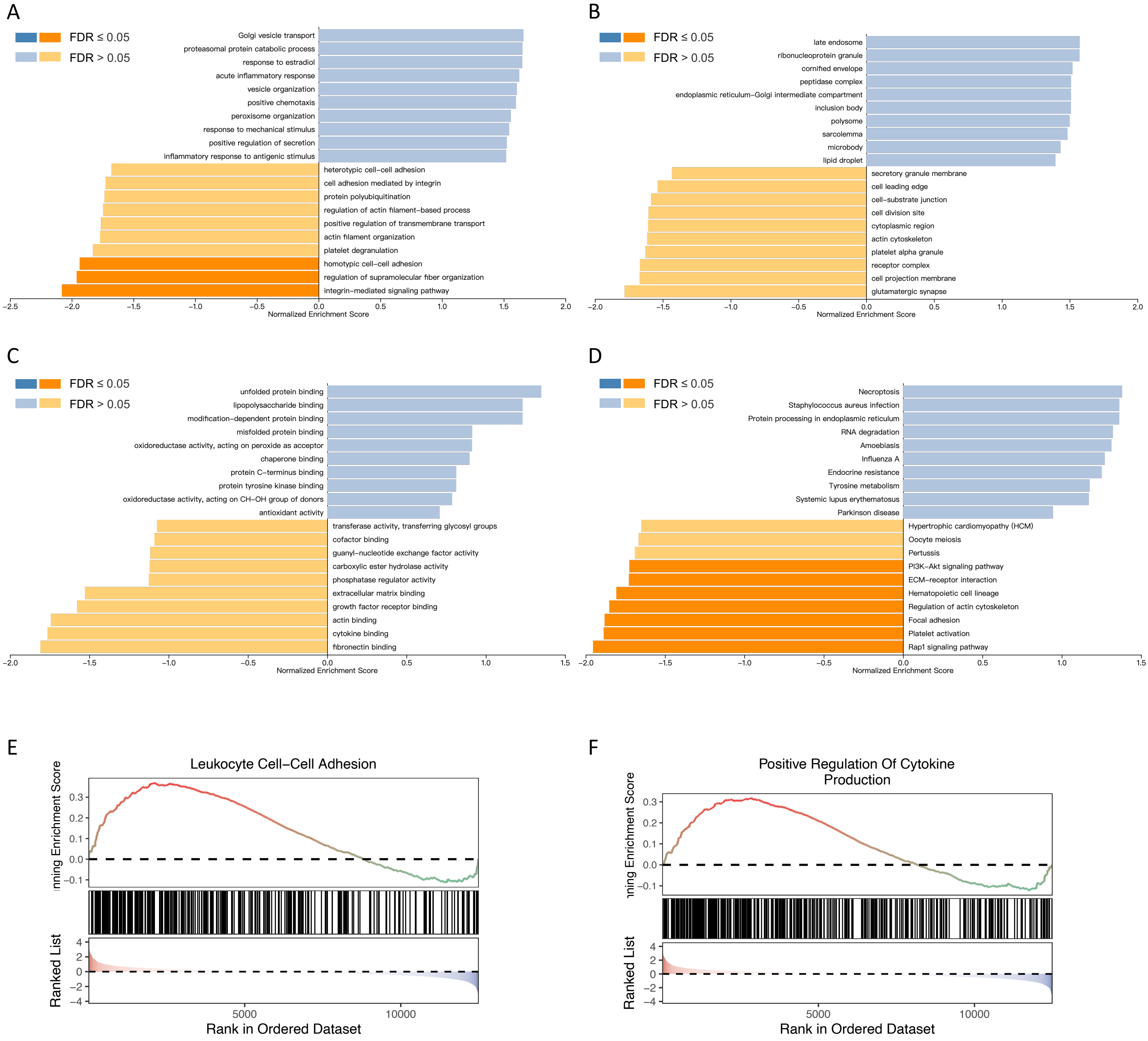
A
FDR ≤ 0.05
FDR > 0.05
Golgi vesicle transport
proteasomal protein catabolic process
response to estradiol
acute inflammatory response
vesicle organization
positive chemotaxis
peroxisome organization
response to mechanical stimulus
positive regulation of secretion
inflammatory response to antigenic stimulus
heterotypic cell–cell adhesion
cell adhesion mediated by integrin
protein polyubiquitination
regulation of actin filament–based process
positive regulation of transmembrane transport
actin filament organization
platelet degranulation
homotypic cell–cell adhesion
regulation of supramolecular fiber organization
integrin–mediated signaling pathway
−2.5
−2.0
−1.5
−1.0
−0.5
0.0
0.5
1.0
1.5
2.0
Normalized Enrichment Score
B
FDR ≤ 0.05
FDR > 0.05
late endosome
ribonucleoprotein granule
cornified envelope
peptidase complex
endoplasmic reticulum–Golgi intermediate compartment
inclusion body
polysome
sarcolemma
microbody
lipid droplet
secretory granule membrane
cell leading edge
cell–substrate junction
cell division site
cytoplasmic region
actin cytoskeleton
platelet alpha granule
receptor complex
cell projection membrane
glutamatergic synapse
−2.0
−1.5
−1.0
−0.5
0.0
0.5
1.0
1.5
2.0
Normalized Enrichment Score
C
FDR ≤ 0.05
FDR > 0.05
unfolded protein binding
lipopolysaccharide binding
modification–dependent protein binding
misfolded protein binding
oxidoreductase activity, acting on peroxide as acceptor
chaperone binding
protein C–terminus binding
protein tyrosine kinase binding
oxidoreductase activity, acting on CH–OH group of donors
antioxidant activity
transferase activity, transferring glycosyl groups
cofactor binding
guanyl–nucleotide exchange factor activity
carboxylic ester hydrolase activity
phosphatase regulator activity
extracellular matrix binding
growth factor receptor binding
actin binding
cytokine binding
fibronectin binding
−2.0
−1.5
−1.0
−0.5
0.0
0.5
1.0
1.5
Normalized Enrichment Score
D
FDR ≤ 0.05
FDR > 0.05
Necroptosis
Staphylococcus aureus infection
Protein processing in endoplasmic reticulum
RNA degradation
Amoebiasis
Influenza A
Endocrine resistance
Tyrosine metabolism
Systemic lupus erythematosus
Parkinson disease
Hypertrophic cardiomyopathy (HCM)
Oocyte meiosis
Pertussis
PI3K–Akt signaling pathway
ECM–receptor interaction
Hematopoietic cell lineage
Regulation of actin cytoskeleton
Focal adhesion
Platelet activation
Rap1 signaling pathway
−2.0
−1.5
−1.0
−0.5
0.0
0.5
1.0
1.5
Normalized Enrichment Score
E
Leukocyte Cell–Cell Adhesion
nning Enrichment Score
0.3
0.2
0.1
0.0
−0.1
Ranked List
4
2
0
−2
−4
5000
10000
Rank in Ordered Dataset
F
Positive Regulation Of Cytokine Production
nning Enrichment Score
0.3
0.2
0.1
0.0
−0.1
Ranked List
4
2
0
−2
−4
5000
10000
Rank in Ordered Dataset

Supplementary Figure 1. Systemic inflammation is elevated in peripheral blood from patients with AD. (A) GSEA of biological processes of differently expressed proteins. (B) GSEA of cellular component in differently expressed proteins. (C) GSEA of molecular function in differently expressed proteins. (D) KEGG analysis in differently expressed proteins. A positive enrichment score indicates association with AD. (E-F) GSEA showed the hallmark pathways enriched in the patients with AD including leukocyte cell-cell adhesion, and positive regulation of cytokine production. **KEGG**: Kyoto encyclopedia of genes and genomes; **GSEA**: Gene set enrichment analysis.

SFigure 2

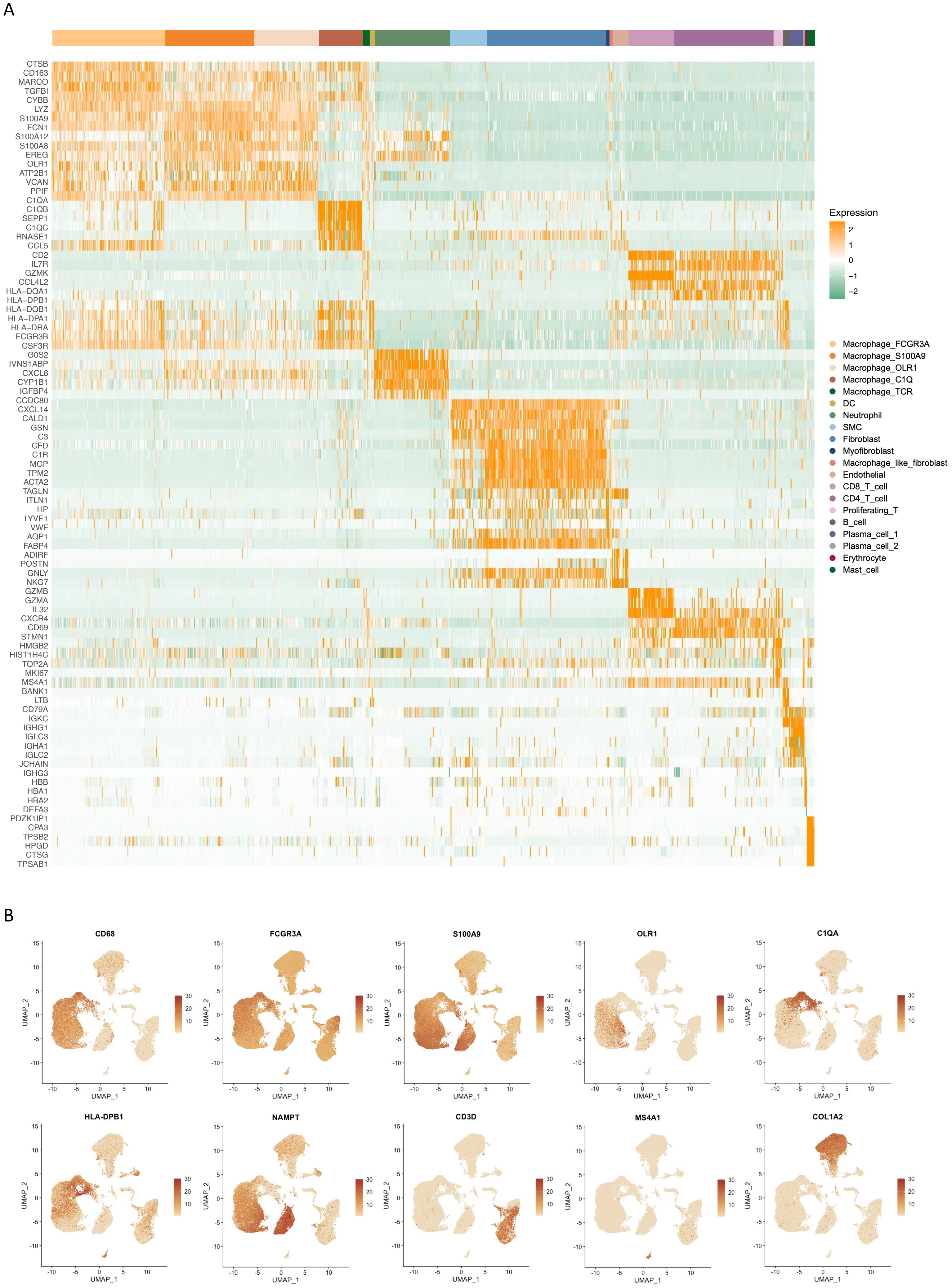
A
CTSB
CD163
MARCO
TGFBI
CYBB
LYZ
S100A9
FCN1
S100A12
S100A8
EREG
OLR1
ATP2B1
VCAN
PPIF
C1QA
C1QB
SEPP1
C1QC
RNASE1
CCL5
CD2
IL7R
GZMK
CCL4L2
HLA−DQA1
HLA−DPB1
HLA−DQB1
HLA−DPA1
HLA−DRA
FCGR3B
CSF3R
G0S2
IVNS1ABP
CXCL8
CYP1B1
IGFBP4
CCDC80
CXCL14
CALD1
GSN
C3
CFD
C1R
MGP
TPM2
ACTA2
TAGLN
ITLN1
HP
LYVE1
VWF
AQP1
FABP4
ADIRF
POSTN
GNLY
NKG7
GZMB
GZMA
IL32
CXCR4
CD69
STMN1
HMGB2
HIST1H4C
TOP2A
MKI67
MS4A1
BANK1
LTB
CD79A
IGKC
IGHG1
IGLC3
IGHA1
IGLC2
JCHAIN
IGHG3
HBB
HBA1
HBA2
DEFA3
PDZK1IP1
CPA3
TPSB2
HPGD
CTSG
TPSAB1
Expression
2
1
0
−1
−2
Macrophage_FCGR3A
Macrophage_S100A9
Macrophage_OLR1
Macrophage_C1Q
Macrophage_TCR
DC
Neutrophil
SMC
Fibroblast
Myofibroblast
Macrophage_like_fibroblast
Endothelial
CD8_T_cell
CD4_T_cell
Proliferating_T
B_cell
Plasma_cell_1
Plasma_cell_2
Erythrocyte
Mast_cell
B
CD68
FCGR3A
S100A9
OLR1
C1QA
HLA-DPB1
NAMPT
CD3D
MS4A1
COL1A2
UMAP_1
UMAP_2
-10
-5
0
5
10
15
30
20
10

Supplementary Figure 2. Single-cell transcriptomic analyses show cell populations with expression patterns in aortic lesions in AD. (A) Heatmap showing the most upregulated genes (ordered by decreasing p-value) in each cluster and selected enriched genes used for biological identification of each cluster (Scale: log2 fold change). (B) Log-transformed gene expression patterns projected onto UMAP plots of CD68, FCGR3A, S100A9, OLR1, C1QA, HLA-DPB1, NAMPT, CD3D, MS4A1, and COL1A2.

SFigure 3

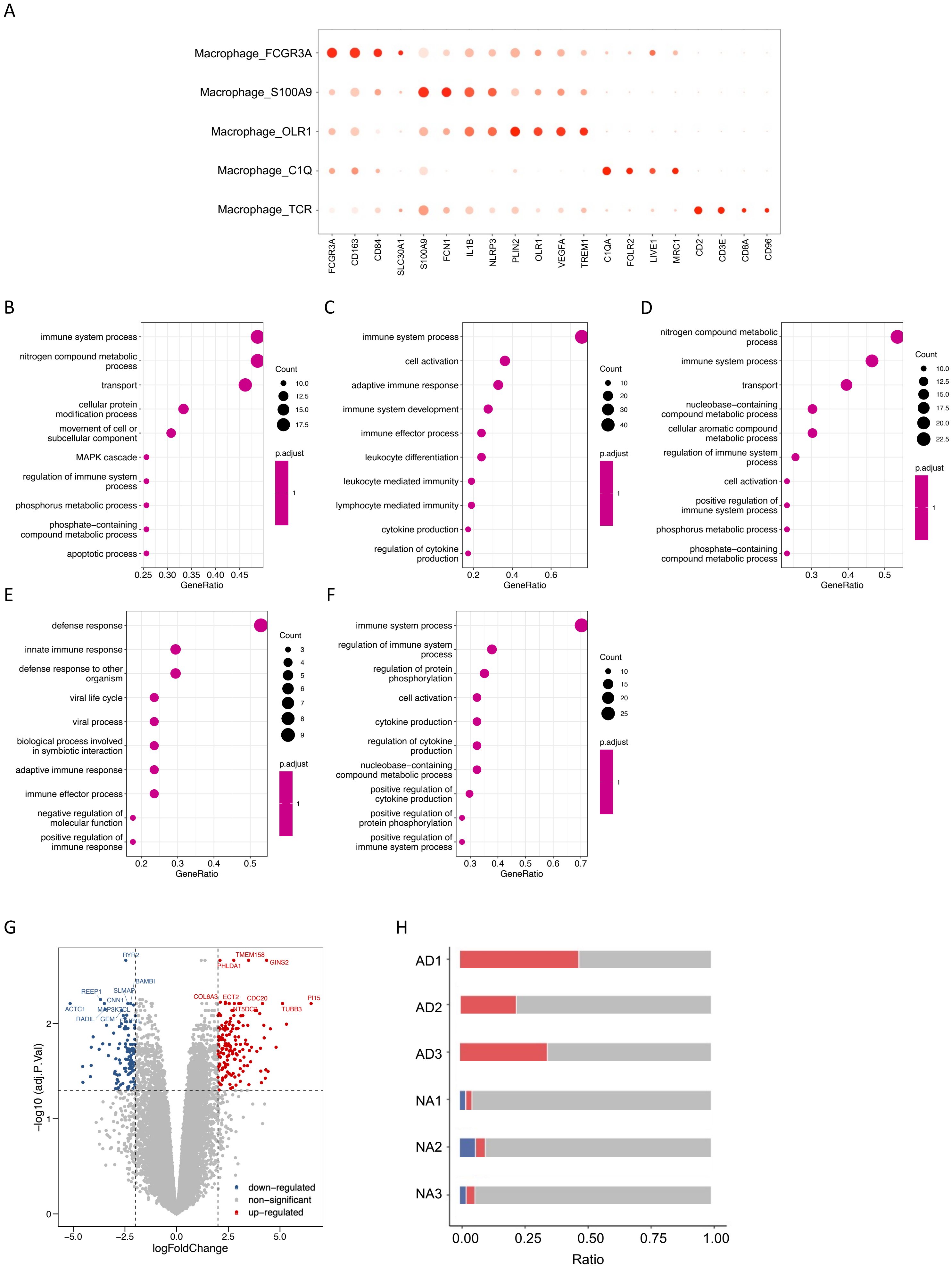
A
Macrophage_FCGR3A
Macrophage_S100A9
Macrophage_OLR1
Macrophage_C1Q
Macrophage_TCR
FCGR3A
CD163
CD84
SLC30A1
S100A9
FCN1
IL1B
NLRP3
PLIN2
OLR1
VEGFA
TREM1
C1QA
FOLR2
LIVE1
MRC1
CD2
CD3E
CD8A
CD96
B
immune system process
nitrogen compound metabolic process
transport
cellular protein modification process
movement of cell or subcellular component
MAPK cascade
regulation of immune system process
phosphorus metabolic process
phosphate−containing compound metabolic process
apoptotic process
0.25
0.30
0.35
0.40
0.45
GeneRatio
Count
10.0
12.5
15.0
17.5
p.adjust
1
C
immune system process
cell activation
adaptive immune response
immune system development
immune effector process
leukocyte differentiation
leukocyte mediated immunity
lymphocyte mediated immunity
cytokine production
regulation of cytokine production
0.2
0.4
0.6
GeneRatio
Count
10
20
30
40
p.adjust
1
D
nitrogen compound metabolic process
immune system process
transport
nucleobase−containing compound metabolic process
cellular aromatic compound metabolic process
regulation of immune system process
cell activation
positive regulation of immune system process
phosphorus metabolic process
phosphate−containing compound metabolic process
0.3
0.4
0.5
GeneRatio
Count
10.0
12.5
15.0
17.5
20.0
22.5
p.adjust
1
E
defense response
innate immune response
defense response to other organism
viral life cycle
viral process
biological process involved in symbiotic interaction
adaptive immune response
immune effector process
negative regulation of molecular function
positive regulation of immune response
0.2
0.3
0.4
0.5
GeneRatio
Count
3
4
5
6
7
8
9
p.adjust
1
F
immune system process
regulation of immune system process
regulation of protein phosphorylation
cell activation
cytokine production
regulation of cytokine production
nucleobase−containing compound metabolic process
positive regulation of cytokine production
positive regulation of protein phosphorylation
positive regulation of immune system process
0.3
0.4
0.5
0.6
0.7
GeneRatio
Count
10
15
20
25
p.adjust
1
G
RYR2
TMEM158
PHLDA1
GINS2
BAMBI
REEP1
SLMAP
CNN1
ACTC1
MAP3K7CL
RADIL
GEM
FILIP1L
COL6A3
ECT2
CDC20
NT5DC2
PI15
TUBB3
2
1
0
−log10 (adj.P.Val)
−5.0
−2.5
0.0
2.5
5.0
logFoldChange
down−regulated
non−significant
up−regulated
H
AD1
AD2
AD3
NA1
NA2
NA3
0.00
0.25
0.50
0.75
1.00
Ratio

Supplementary Figure 3. Single-cell transcriptomic analyses show cell populations with putative functions in aortic lesions in AD. (A) Dotplot of log-transformed gene expression of selected genes showing statistically significant upregulation in inflammatory macrophages (Macrophage_FCGR3A), atherosclerosis-like macrophages (Macrophage_OLR1), MDSCs-like macrophages (Macrophage_S100A9), tissue resident macrophages (Macrophage_C1Q), TCR$^+$ macrophages (Macrophage_TCR). (B) Gene ontology enrichment analysis of biological processes in FCGR3A$^+$ macrophages in single-cell sequencing data. (C) Gene ontology enrichment analysis of biological processes in MSDCs-like macrophages in single-cell sequencing data. (D) Gene ontology enrichment analysis of biological processes in OLR1$^+$ macrophages in single-cell sequencing data. (E) Gene ontology enrichment analysis of biological processes in tissue resident macrophages in single-cell sequencing data. (F) Gene ontology enrichment analysis of biological processes in TCR$^+$ macrophages in single-cell sequencing data. (G) Volcano plot shows the differentially expressed genes between patients with AD (n = 7) and healthy individuals (n = 5) from a publicly available bulk RNA-seq dataset (GSE52093). (H) Histogram indicates the proportion of Scissor-selected cells in aortic tissue of each analyzed patient with AD ($n = 3$) and healthy individual ($n = 3$). A two-sided statistical significance was set at adjusted $p < 0.05$. **AD**: aortic dissection; **FCGR3A**: Fc fragment of IgG receptor 3a; **MDSCs**: myeloid-derived suppressor cells; **S100A9**: S100 calcium binding protein A9; **OLR1**: oxidized low density lipoprotein receptor 1.

SFigure 4

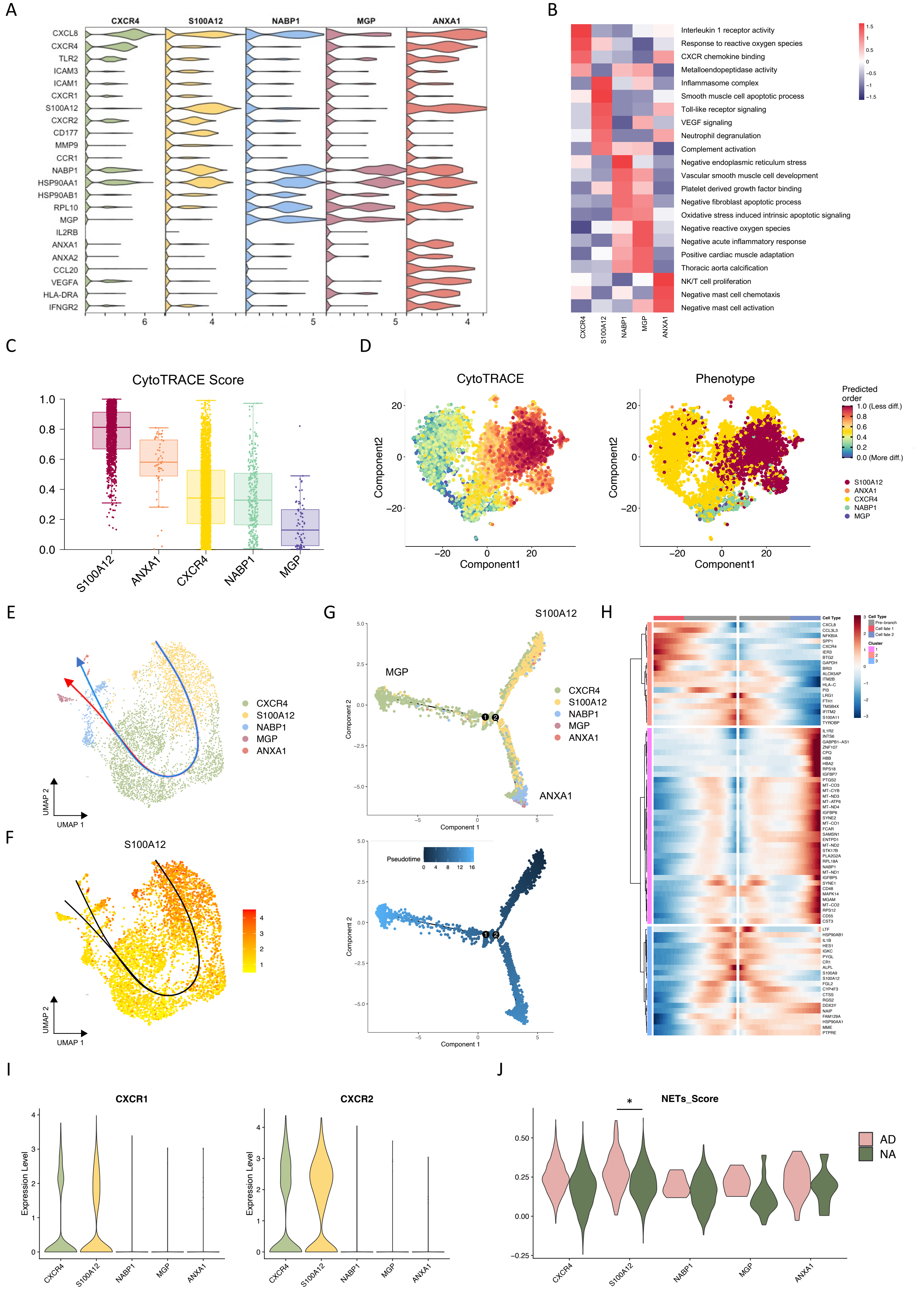
A
CXCR4
S100A12
NABP1
MGP
ANXA1
CXCL8
CXCR4
TLR2
ICAM3
ICAM1
CXCR1
S100A12
CXCR2
CD177
MMP9
CCR1
NABP1
HSP90AA1
HSP90AB1
RPL10
MGP
IL2RB
ANXA1
ANXA2
CCL20
VEGFA
HLA-DRA
IFNGR2
6
4
5
5
4
B
Interleukin 1 receptor activity
Response to reactive oxygen species
CXCR chemokine binding
Metalloendopeptidase activity
Inflammasome complex
Smooth muscle cell apoptotic process
Toll-like receptor signaling
VEGF signaling
Neutrophil degranulation
Complement activation
Negative endoplasmic reticulum stress
Vascular smooth muscle cell development
Platelet derived growth factor binding
Negative fibroblast apoptotic process
Oxidative stress induced intrinsic apoptotic signaling
Negative reactive oxygen species
Negative acute inflammatory response
Positive cardiac muscle adaptation
Thoracic aorta calcification
NK/T cell proliferation
Negative mast cell chemotaxis
Negative mast cell activation
CXCR4
S100A12
NABP1
MGP
ANXA1
1.5
1
0.5
0
−0.5
−1
−1.5
C
CytoTRACE Score
1.0
0.8
0.6
0.4
0.2
0.0
S100A12
ANXA1
CXCR4
NABP1
MGP
D
CytoTRACE
Phenotype
Component2
Component1
20
0
−20
−20
0
20
Predicted order
1.0 (Less diff.)
0.8
0.6
0.4
0.2
0.0 (More diff.)
S100A12
ANXA1
CXCR4
NABP1
MGP
E
CXCR4
S100A12
NABP1
MGP
ANXA1
UMAP 2
UMAP 1
F
S100A12
4
3
2
1
UMAP 2
UMAP 1
G
S100A12
MGP
ANXA1
CXCR4
S100A12
NABP1
MGP
ANXA1
Component 2
Component 1
5.0
2.5
0.0
−2.5
−5.0
−5
0
5
1
2
Pseudotime
0
4
8
12
16
H
Cell Type
CXCL8
CCL3L3
NFKBIA
SPP1
CXCR4
IER3
BTG2
GAPDH
BRI3
ALOX5AP
ITM2B
HLA−C
PI3
LRG1
FTH1
TMSB4X
IFITM2
S100A11
TYROBP
IL1R2
INTS6
GABPB1−AS1
ZNF107
CPQ
HBB
HBA2
RPS18
IGFBP7
PTGS2
MT−CO3
MT−CYB
MT−ND3
MT−ATP6
MT−ND4
IGFBP6
SYNE2
MT−CO1
FCAR
SAMSN1
ENTPD1
MT−ND2
STK17B
PLA2G2A
RPL18A
NABP1
MT−ND1
IGFBP5
SYNE1
CD48
MAPK14
MGAM
MT−CO2
RPS12
CD55
CST3
LTF
HSP90AB1
IL1B
HES1
IGKC
PYGL
CR1
ALPL
S100A9
S100A12
FGL2
CYP4F3
CTSS
RGS2
DDX3Y
NAIP
FAM129A
HSP90AA1
MME
PTPRE
3
2
1
0
−1
−2
−3
Cell Type
Pre−branch
Cell fate 1
Cell fate 2
Cluster
1
2
3
I
CXCR1
CXCR2
Expression Level
4
3
2
1
0
CXCR4
S100A12
NABP1
MGP
ANXA1
J
NETs_Score
*
0.50
0.25
0.00
−0.25
CXCR4
S100A12
NABP1
MGP
ANXA1
AD
NA

Supplementary Figure 4. Neutrophil heterogeneity and differentiation trajectories. (A) Violin plot showing the expression levels of markers of each subset. (B) Heatmap showing the scale normalized gene set enrichment analysis (GSVA) scores for select Gene Ontology pathways in each neutrophil subset. (C) Boxplot showing the comparison of CytoTRACE score among different neutrophil subsets. (D) Cell differentiation ordered by CytoTRACE score projected on UMAP plot. (E) Neutrophil subsets projected on UMAP plot with bifurcating differentiation trajectories by Slingshot (red and blue smooth lines). (F) The expression of S100A12 in neutrophil subsets projected on UMAP plot. (G-H) trajectory and heatmap of neutrophils with markers by Monocle. (I) Violin plot showing the expression of CXCR1 and CXCR2. (J) NETs-associated gene module score of neutrophil subsets in AD and normal aortas.

SFigure 5

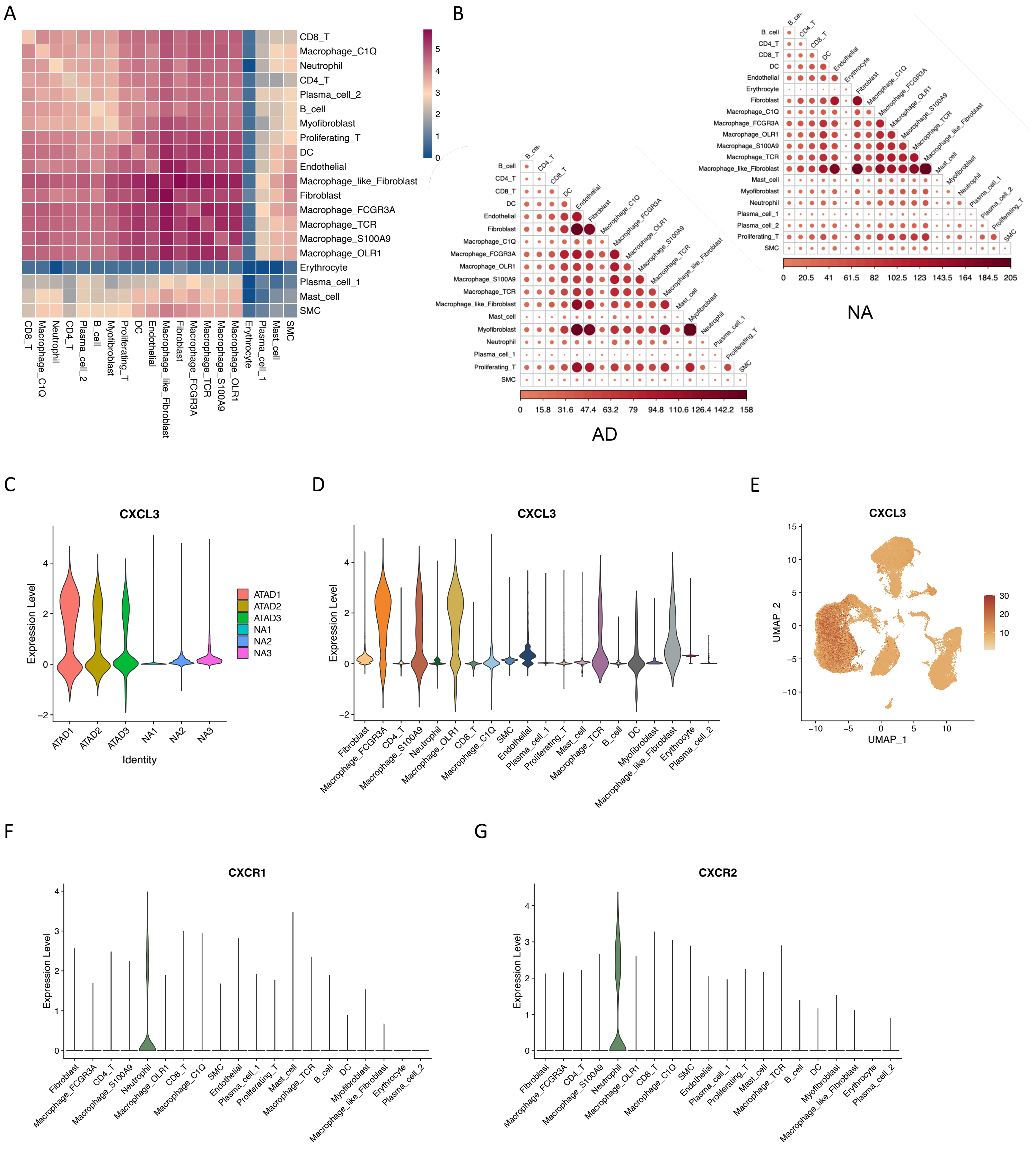
A
CD8_T
Macrophage_C1Q
Neutrophil
CD4_T
Plasma_cell_2
B_cell
Myofibroblast
Proliferating_T
DC
Endothelial
Macrophage_like_Fibroblast
Fibroblast
Macrophage_FCGR3A
Macrophage_TCR
Macrophage_S100A9
Macrophage_OLR1
Erythrocyte
Plasma_cell_1
Mast_cell
SMC
5
4
3
2
1
0
B
AD
0
15.8
31.6
47.4
63.2
79
94.8
110.6
126.4
142.2
158
NA
0
20.5
41
61.5
82
102.5
123
143.5
164
184.5
205
C
CXCL3
Expression Level
Identity
ATAD1
ATAD2
ATAD3
NA1
NA2
NA3
D
CXCL3
Expression Level
E
CXCL3
UMAP_1
UMAP_2
30
20
10
F
CXCR1
Expression Level
G
CXCR2
Expression Level
Fibroblast
Macrophage_FCGR3A
CD4_T
Macrophage_S100A9
Neutrophil
Macrophage_OLR1
CD8_T
Macrophage_C1Q
SMC
Endothelial
Plasma_cell_1
Proliferating_T
Mast_cell
Macrophage_TCR
B_cell
DC
Myofibroblast
Macrophage_like_Fibroblast
Erythrocyte
Plasma_cell_2

Supplementary Figure 5. Cell-cell interactions in aortic lesions in AD. (A) Cellphone DB analysis shows the number of ligand-receptor interactions between all cell populations. (B) Cellphone DB analysis shows the difference of number of ligand-receptor interactions between all cell populations across patients with AD and healthy individuals. (C) Violin plot showing the expression level of CXCL3 between patients with AD and healthy individuals. (D) Violin plot showing the expression level of CXCL3 among all cell populations. (E) The expression level of CXCL3 projected on UMAP plot. (F) Violin plot showing the expression level of CXCR1 among all cell populations. (G) Violin plot showing the expression level of CXCR2 among all cell populations. A two-sided statistical significance was set at adjusted $p < 0.05$.

SFigure 6

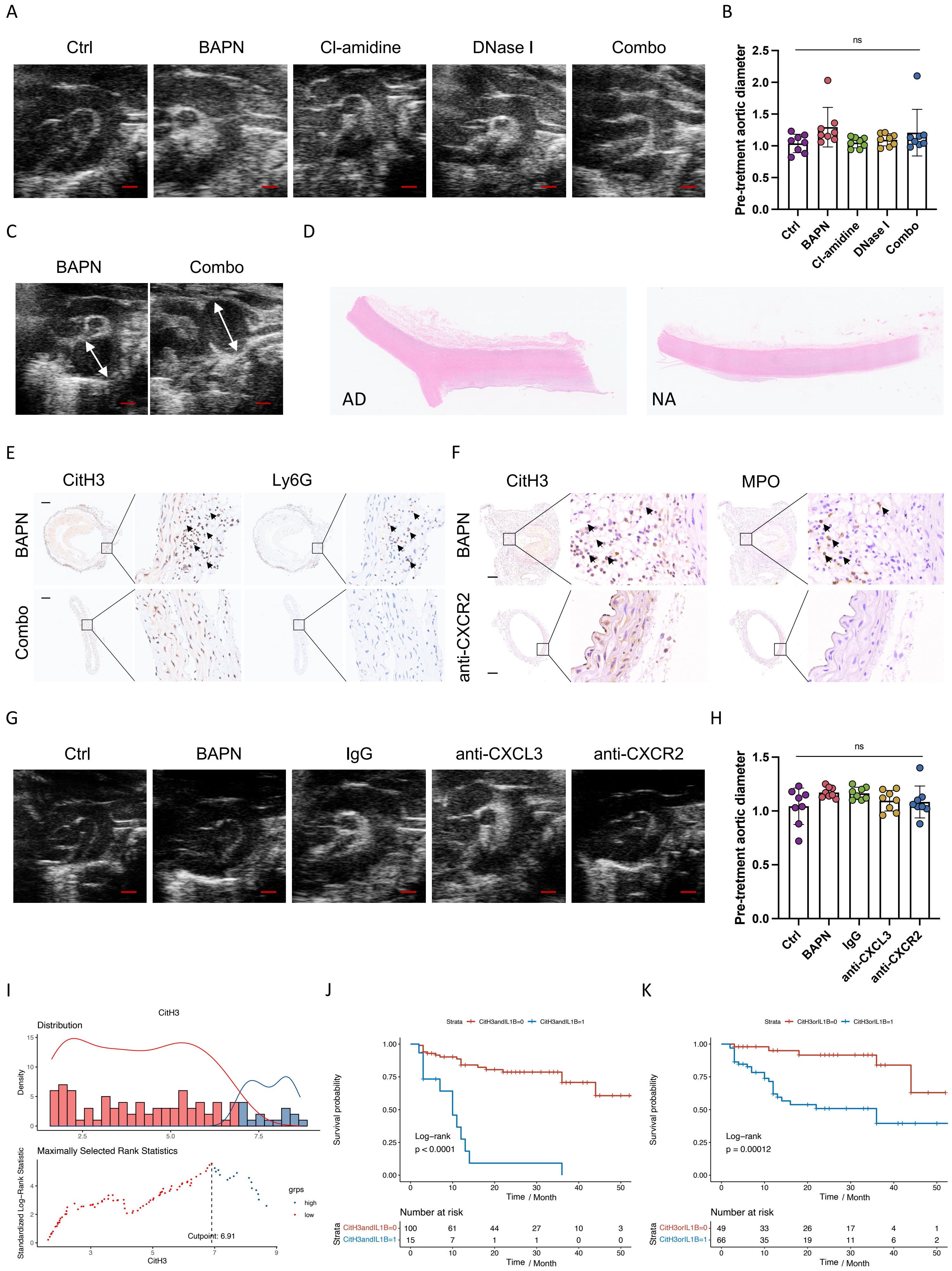
A
Ctrl
BAPN
Cl-amidine
DNase I
Combo
B
ns
Pre-tretment aortic diameter
2.5
2.0
1.5
1.0
0.5
0.0
Ctrl
BAPN
Cl-amidine
DNase I
Combo
C
BAPN
Combo
D
AD
NA
E
CitH3
Ly6G
BAPN
Combo
F
CitH3
MPO
BAPN
anti-CXCR2
G
Ctrl
BAPN
IgG
anti-CXCL3
anti-CXCR2
H
ns
Pre-tretment aortic diameter
1.5
1.0
0.5
0.0
Ctrl
BAPN
IgG
anti-CXCL3
anti-CXCR2
I
CitH3
Distribution
Density
15
10
5
0
2.5
5.0
7.5
Maximally Selected Rank Statistics
Standardized Log−Rank Statistic
4
2
0
3
5
7
9
CitH3
Cutpoint: 6.91
grps
high
low
J
Strata
CitH3andIL1B=0
CitH3andIL1B=1
Survival probability
1.00
0.75
0.50
0.25
0.00
Log−rank
p < 0.0001
0
10
20
30
40
50
Time / Month
Number at risk
Strata
CitH3andIL1B=0 100 61 44 27 10 3
CitH3andIL1B=1 15 7 1 1 0 0
0
10
20
30
40
50
Time / Month
K
Strata
CitH3orIL1B=0
CitH3orIL1B=1
Survival probability
1.00
0.75
0.50
0.25
0.00
Log−rank
p = 0.00012
0
10
20
30
40
50
Time / Month
Number at risk
Strata
CitH3orIL1B=0 49 33 26 17 4 1
CitH3orIL1B=1 66 35 19 11 6 2
0
10
20
30
40
50
Time / Month

Supplementary Figure 6. Inhibition of NETs attenuates dissection progression in mice with AD. (A) Representative pre-treatment vascular ultrasound images of aorta in each group. Scale bar = 1 mm. (B) Baseline aortic diameters of each mouse measured by vascular ultrasound at day 7 before the administration of NETs inhibitors. (C) Representative images of two mice with enlarged section located in proximal descending aorta (indicated by white arrow) in BAPN and combination treatment groups. Scale bar = 1 mm. (D) The H&E images show the longitudinal section of dissected and normal aortas. H&E: hematoxylin and eosin. (E-F) The immunohistochemistry images showing NETs formation within aortas in mice with BAPN and NETs inhibition, determined by staining of CitH3 and Ly6G, and CitH3 and MPO, respectively. Scale bar = 100 μm. (G) Representative pre-treatment vascular ultrasound images of aorta in each group. Scale bar = 1 mm. (H) Baseline aortic diameters of each mouse measured by vascular ultrasound at day 7 before the administration of anti-CXCL3 and anti-CXCR2 antibodies. (I) The maximally selected log-rank statistic indicates the cut-off value of CitH3 level. (J) Kaplan-Meier curves of patients with both high CitH3 (≥ 6.91 ng/ml) and high IL-1β (≥ 90.86 pg/ml) compared to remaining patients. Below the survival curves showing the number of exposed subjects at each time point. (K) Kaplan-Meier curves of patients with either high CitH3 (≥ 6.91 ng/ml) or high IL-1β (≥ 90.86 pg/ml). Below the survival curves showing the number of exposed subjects at each time point. $^{*}p < 0.05$, $^{**}p < 0.01$, $^{***}p < 0.001$, $^{****}p < 0.0001$ by Mann-Whitney U test.

Supplementary Table 1. Baseline characteristics of patients with AD and healthy individuals involved in mass spectrometry.

	AD (N = 30)	CL (N = 30)	P-value
Age (y)	57.1 ± 12.0	52.8 ± 8.1	0.113†
Gender			1‡
M	27 (90.0%)	27 (90.0%)	
F	3 (10.0%)	3 (10.0%)	
Hypertension	21 (70.0%)	0	< .001‡
Smoking	11 (36.7%)	0	< .001‡
Diabetes mellitus	5 (16.7%)	0	0.052‡
Alcohol abuse	13 (53.3%)	0	< .001‡
Stroke	2 (6.7%)	0	0.491‡
Coronary heart disease	6 (20%)	0	0.023‡
Chronic kidney disease	0	0	1‡
Neutrophil ($\times 10^9$ /L)	7.0 ± 2.1	3.8 ± 0.8	< .001†
Monocyte ($\times 10^9$ /L)	0.8 ± 0.4	0.6 ± 0.6	0.189†
Lymphocyte ($\times 10^9$ /L)	1.3 ± 0.5	2.0 ± 0.9	0.006†
Platelet ($\times 10^9$ /L)	234.9 ± 93.5	259.9 ± 54.4	0.260†
D-dimer (mg/L)	5.1 ± 5.2	0.2 ± 0.1	< .001†
ALT (U/L)	29.7 ± 38.4	34.8 ± 16.9	0.542†
AST (U/L)	23.1 ± 19.8	27.7 ± 7.3	0.272†
Cholesterol (mmol/L)	4.7 ± 1.0	5.2 ± 0.6	0.115†
Triglyceride (mmol/L)	1.2 ± 0.4	1.9 ± 0.6	0.001†

† Mann-Whitney test

‡ Fisher's exact test

Values are expressed as means ± SD.

ALT: Alanine transaminase; **AST**: Aspartate aminotransferase.

Supplementary Table 2. Baseline characteristics of patients with AD and healthy individuals in diagnostic cohort.

	AD (N = 187)	CL (N = 59)	P-value
Gender			<.001‡
M	29 (15.5%)	27 (45.8%)	
F	158 (84.5%)	32 (54.2%)	
Age	56.6 ± 13.6	46.7 ± 14.6	<.001†
D-dimer	4.5 ± 5.2	3.6 ± 5.1	0.227†
WBC ($\times 10^9$ /L)	7.5 ± 4.4	7.3 ± 1.8	0.459†
Neutrophil ($\times 10^9$ /L)	6.4 ± 2.6	4.4 ± 2.2	<.001†
Monocyte ($\times 10^9$ /L)	0.8 ± 0.8	0.4 ± 0.2	<.001†
Lymphocyte ($\times 10^9$ /L)	1.3 ± 0.5	2.4 ± 0.6	<.001†
Platelet ($\times 10^9$ /L)	202.3 ± 71.1	255.7 ± 65.2	<.001†
Albumin (g/L)	40.7 ± 4.8	46.2 ± 2.7	<.001†
Creatinine (μmol/L)	91.9 ± 92.2	74.0 ± 17.2	0.012†
GFR (ml/min)	71.3 ± 32.6	81.3 ± 30.0	0.038†
Cholesterol (mmol/L)	4.1 ± 1.1	4.8 ± 1.0	<.001†
Triglyceride (mmol/L)	1.4 ± 0.9	1.5 ± 1.4	0.646†
LDL (mmol/L)	2.3 ± 0.8	3.2 ± 0.9	<.001†
HDL (mmol/L)	1.4 ± 0.9	1.2 ± 0.3	0.010†
CRP (mg/L)	56.5 ± 52.7	45.7 ± 49.2	0.165†
CitH3 (ng/mL)	4.4 ± 3.0	1.8 ± 1.3	<.001†
cf-DNA (ng/mL)	2.0 ± 0.7	1.7 ± 0.6	0.006†
MPO (ng/mL)	4.4 ± 2.5	2.8 ± 1.7	<.001†
NE (ng/mL)	4.1 ± 1.9	2.2 ± 1.3	<.001†
IL-1β (pg/mL)	94.2 ± 29.0	86.6 ± 26.7	0.074†
IL-6 (pg/mL)	45.2 ± 19.7	37.7 ± 17.4	0.010†
Hypertension	146 (78.1%)	3 (1.6%)	<.001‡
Smoking	106 (56.7%)	3 (1.6%)	<.001‡
Alcohol abuse	80 (42.8%)	3 (1.6%)	<.001‡
Diabetes mellitus	75 (40.1%)	3 (1.6%)	<.001‡
Coronary heart disease	8 (4.3%)	0	0.204‡
Stroke	1 (0.5%)	0	1‡
Chronic kidney disease	8 (4.3%)	0	0.204‡

† Mann-Whitney test

‡ Fisher's exact test

Values are expressed as means ± SD.

WBC: White blood cell; **GFR**: Glomeruar filtration rate; **LDL**: Low density lipoprotein; **HDL**: High density lipoprotein; **CRP**: C-reactive protein; **CitH3**: citrullinated histone H3; **cf-DNA**: cell free-DNA; **MPO**: myeloperoxidase; **NE**: Neutrophil elastase.

Supplementary Table 3. LASSO and multivariable logistic regression analyses of patients with AD and healthy individuals in diagnostic cohort.

	OR (95% CI)	P-value
Gender	1.98 (0.37-10.75)	.416
Age	1.01 (0.96-1.07)	.638
Neutrophil	0.75 (0.53-1.03)	.079
Monocyte	7.36 (1.71-9.67)	< .001
Lymphocyte	0.79 (0.10-0.89)	< .001
Platelet	0.99 (0.98-1.01)	.325
LDL	0.41 (0.18-0.87)	.025
HDL	1.03 (0.42-4.10)	.952
CRP	1.00 (0.99-1.01)	.976
CitH3	2.02 (1.39-3.38)	.002
cf-DNA	0.84 (0.22-3.20)	.791

LDL: Low density lipoprotein; **HDL**: High density lipoprotein; **CRP**: C-reactive protein; **CitH3**: citrullinated histone H3; **cf-DNA**: cell free-DNA.

Supplementary Table 4. Baseline characteristics of patients with AD receiving TEVAR in predicting AAEs.

		non-AAEs (N=85)	AAEs (N=31)	P-value
Age		56.2 ± 13.7	54.0 ± 14.5	0.468†
Gender				0.077‡
	Female	12 (14.1%)	10 (32.3%)	
	Male	72 (84.7%)	21 (67.7%)	
Phase				0.328‡
	Acute	70 (82.4%)	22 (71%)	
	Subacute	9 (10.6%)	4 (12.9%)	
	Chronic	4 (4.7%)	2 (6.5%)	
D-dimer		4.5 ± 5.1	7.2 ± 7.0	0.056†
Neutrophil		6.3 ± 2.6	7.2 ± 2.4	0.088†
Monocyte		0.7 ± 0.3	0.7 ± 0.3	0.413†
Lymphocyte		1.3 ± 0.4	1.2 ± 0.4	0.366†
Platelet		211.4 ± 79.5	192.1 ± 70.8	0.238†
Albumin		40.5 ± 4.4	40.5 ± 3.5	0.970†
Cholesterol		4.1 ± 1.2	4.1 ± 0.7	0.734†
Triglyceride		1.4 ± 0.9	1.1 ± 0.5	0.036†
LDL		2.2 ± 0.8	2.4 ± 0.6	0.101†
HDL		1.5 ± 1.1	1.3 ± 0.9	0.267†
NLR		5.0 ± 3.2	6.2 ± 3.4	0.086†
PLR		166.8 ± 66.3	179.7 ± 69.8	0.362†
MLR		4.3 ± 3.0	5.0 ± 2.4	0.234†
SII		1014.1 ± 702.5	1163.4 ± 572.1	0.291†
SIRI		0.6 ± 0.2	0.7 ± 0.3	0.018†
CitH3		4.3 ± 2.4	6.9 ± 3.2	<.001†
cf-DNA		2.0 ± 0.6	2.0 ± 0.7	0.650†
MPO		4.8 ± 2.3	6.0 ± 2.5	0.020†
NE		4.1 ± 1.9	4.2 ± 1.7	0.834†
IL-1β		94.9 ± 29.1	93.0 ± 26.8	0.755†
IL-6		43.8 ± 20.0	43.5 ± 17.6	0.946†

† Mann-Whitney test

‡ Fisher's exact test

Values are expressed as means ± SD.

LDL: Low density lipoprotein; **HDL**: High density lipoprotein; **NLR**: Neutrophil-to-lymphocyte ratio; **MLR**: Monocyte-to-lymphocyte ratio; **PLR**: Platelet-to-lymphocyte ratio; **SII**: Systemic immune inflammation index; **SIRI**: Systemic inflammatory response index; **CitH3**: citrullinated histone H3; **cf-DNA**: cell free-DNA; **MPO**: myeloperoxidase; **NE**: Neutrophil elastase.

Supplementary Table 5. Univariable and multivariable Cox proportional hazard regression analyses of patients receiving TEVAR in predicting AAEs.

	Univariable		Multivariable	
	HR (95% CI)	P-value	HR (95% CI)	P-value
D-dimer	1.04 (1.00-1.09)	.049	1.02 (0.97-1.07)	.510
Neutrophil	1.17 (1.03-1.33)	.017	1.13 (0.95-1.35)	.174
NLR	1.13 (1.04-1.22)	.004	1.07 (0.87-1.30)	.524
MLR	1.14 (1.04-1.25)	.007	0.89 (0.68-1.16)	.379
SIRI	15.33 (3.82-61.53)	.001	14.23 (1.82-111.31)	.011
CitH3	1.24 (1.11-1.37)	< .001	1.18 (1.05-1.33)	.004
MPO	1.18 (1.01-1.39)	.036	1.02 (0.84-1.23)	.847

NLR: Neutrophil-to-lymphocyte ratio; **MLR**: Monocyte-to-lymphocyte ratio; **SIRI**: Systemic inflammatory response index; **CitH3**: citrullinated histone H3; **MPO**: myeloperoxidase.